Nuclear Instruments and Methods in Physics Research A 652 (2011) 216–220

Contents lists available at ScienceDirect

Nuclear Instruments and Methods in Physics Research A

journal homepage: www.elsevier.com/locate/nima

Results from an investigation of the physical origins of nonproportionality in CsI(Tl)

S. Asztalos *, W. Hennig, W.K. Warburton

XIA LLC, 31057 Genstar Road, Hayward, CA 94544, USA

ARTICLE INFO

Available online 29 April 2011

Keywords:
Nonproportionality
CsI(Tl)
Impurities
X-ray fluorescence

ABSTRACT

The relative scintillation response per energy deposited by Compton electrons, or nonproportionality, has traditionally been considered an intrinsic scintillator property. However, such an interpretation is inconsistent with recent results that show nonproportionality to depend on external factors such as shaping time, temperature and supplier. Apparently, at least some of the overall nonproportionality has an extrinsic origin. In this work we describe the results from a suite of measurements designed to test the hypothesis that nonproportionality in CsI(Tl) material has an extrinsic component that correlates with impurity levels. Our choice of material was motivated by the excellent energy resolution observed in one bulk crystal (6.4%)—a marked departure from that measured with conventional CsI(Tl) stock (8–8.5%). Six bulk CsI(Tl) crystals were procured and diced into 44 wafers. Using X-ray fluorescence techniques no conclusive evidence for impurities was found in any of the wafers at the 1–50 ppm level. One crystal exhibited a distinct correlation among energy resolution, decay lifetimes, nonproportionality and a very low level of Tl doping.

© 2011 Elsevier B.V. All rights reserved.

1. Introduction

The relative scintillation response per energy deposited by Compton electrons, or nonproportionality, has traditionally been considered an intrinsic scintillator property. However, support for this interpretation is increasingly untenable in light of measurements that have shown nonproportionality to depend on external factors, such as shaping time and temperature [1]. Consequently, notions on the origin of nonproportionality have evolved to the present moment, where it is gradually acknowledged that at least some of the overall nonproportionality is not an intrinsic scintillator property. The primary goal of this work was to observe correlations between nonproportionality and impurities (an extrinsic property) at the bulk crystal level. A secondary (and more subtle) goal was simultaneously pursued to explore whether sub-crystal variation in impurity levels contributed to bulk crystal nonproportionality. Our choice of CsI(Tl) material was driven by the excellent resolution seen with one crystal (~6.4%)—a marked departure from that documented for conventional CsI(Tl) stock (8–8.5%). This disparity suggests that nonproportionality should originate from impurities and these impurities should be controllable, then there exists the exciting possibility that the resolution of CsI(Tl) could be engineered to achieve 2% resolution, i.e., comparable to $LaBr_3$. Since CsI(Tl) is very widely disseminated, such an improvement could potentially revolutionize the nonproliferation efforts as well as nuclear, particle and medical physics.

2. Measurements

To test the hypothesis that nonproportionality is due, in part, to impurities we obtained six bulk crystals from five growers

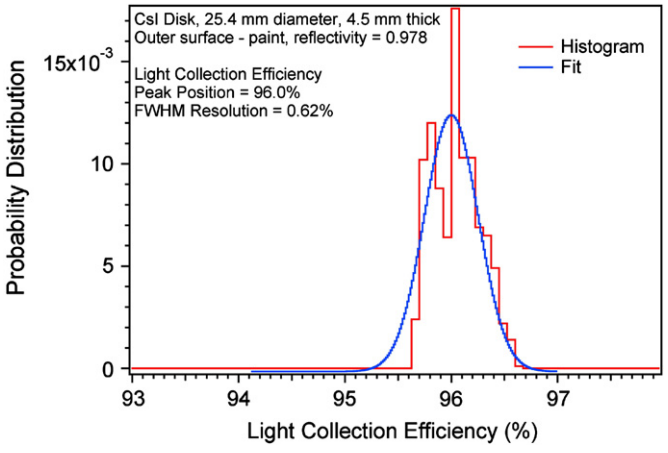

Fig. 1. Probability of light collection from a disk of CsI material with dimensions 4.5 mm × 1.0 in. All surfaces were assumed to have 98% reflectivity.

* Corresponding author. Tel.: +1 510 508 6548.
E-mail address: steve@xia.com (S. Asztalos).

0168-9002/$ - see front matter © 2011 Elsevier B.V. All rights reserved.
doi:10.1016/j.nima.2011.01.164

worldwide (to preserve anonymity concerning growth methods these crystals are subsequently referred to by supplier designations A, B, C, D, D′ and E, with the redundant use of D and D′ denoting two crystals provided by the same supplier). Guided by ray trace simulations (Fig. 1) we converged on a wafer geometry that would simultaneously provide good light collection, minimize a geometric contribution to energy resolution and be readily wrapped and positionable. Each of the six bulk crystals was then diced into 4–9 mm × 4.5 mm × 1 mm in wafers to explore whether wafer variability contributes significantly to overall crystal performance.

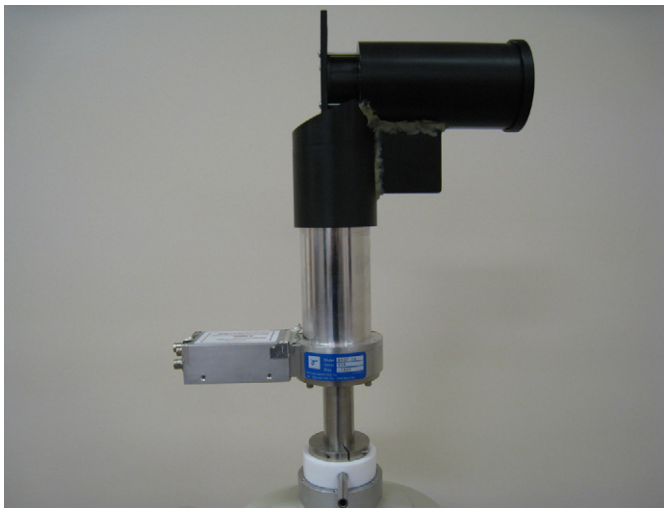

Fig. 2. Customized mounting rig used for CsI(Tl) nonproportionality and decay lifetime measurements. The rig slides over the top of the vertically positioned germanium detector (PGT NIGC 10) and is held in place by mechanical stops. The horizontally mounted PMT (Hamamatsu R329) is positioned such that the CsI(Tl) crystal lying directly above the germanium can centerline. Up to three sources are accommodated by a source holder that can be vertically repositioned to adjust the count rate and geometric scattering angle.

A dedicated mounting rig (Fig. 2) was designed and built to ensure highly reproducible coupling between the wafers and PMT surface. Nonproportionality, energy resolution, decay lifetimes measurements and X-ray fluorescence (XRF) measurements were performed on each of the 44 samples using one mounting rig.

2.1. Nonproportionality

A pair of 5 μ Ci ^{137}Cs sources was used to excite the CsI(Tl) wafers optically coupled to the horizontal PMT (Fig. 2). An XIA Pixie-4 spectrometer recorded coincidence events comprised of the energy of a Compton-scattered photon measured in the germanium detector and that of the energy from light generated by the recoiling electron measured by the PMT. (The sum of these energies of these coincident events is equal to that of the source energy—662 keV. The energy of the recoiling electron is derived by subtracting the energy deposited in the germanium detector from the source energy.) A 1000 ns coincidence window allowed sufficient random coincidences to pass such that energy resolution measurements could be extracted directly from the data sets without the need for a separate calibration run. Data were written to disk in 10 min intervals and corrected offline for PMT and germanium gain drift. Pixie-4 software designed for phoswich detector applications [2] was used to construct calibrated 2D coincidence matrices formed by co-adding ~25–30 data files collectively comprising 2×10^6 events. To keep bin-to-bin fluctuation small these sparse matrices were compressed by a factor of ~50, culminating finally in a 600 × 600 bin 2D matrix with a resolution of 1.6 keV/bin. 1D matrices were constructed by projecting along the axis representing the recoiling electron energy. Local maxima in these projections were fit with a Gaussian and the centroid of the Gaussian fit recorded.

2.2. Decay lifetimes

A Golden Engineering XR-200 X-ray generator with a peak output of around 40 keV and 55 ns pulse width was used to excite

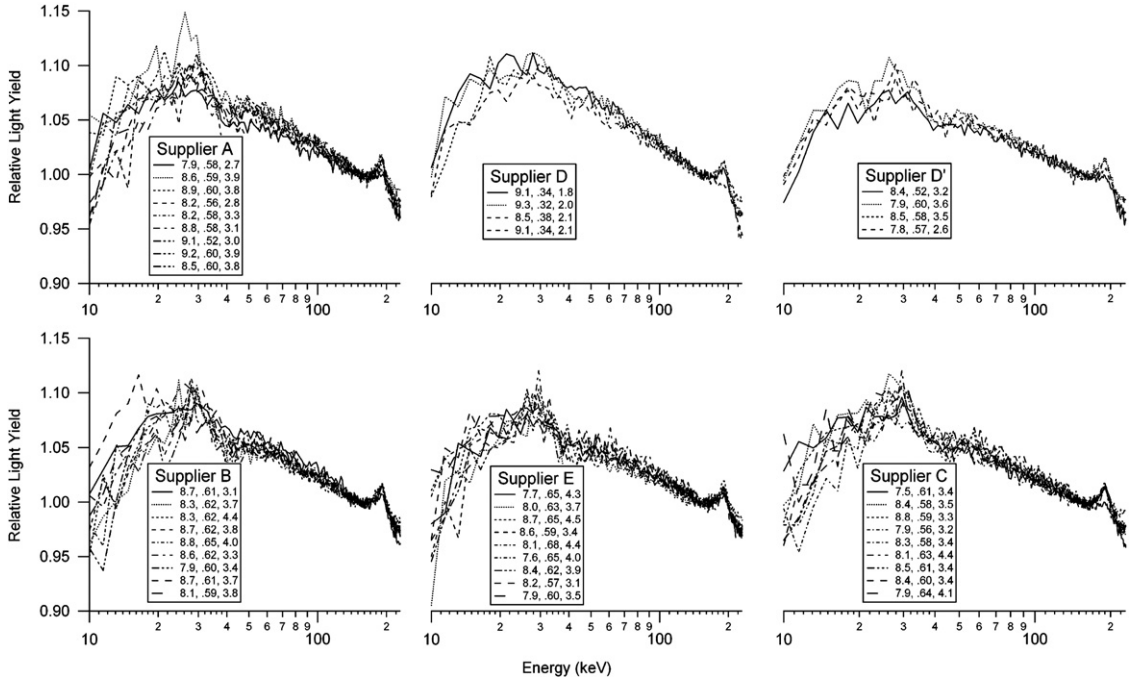

Fig. 3. Nonproportionality for all 44 samples grouped by supplier over the energy interval 10–200 keV. Each curve is normalized by its relative light yield over the energy interval 160–170 keV.

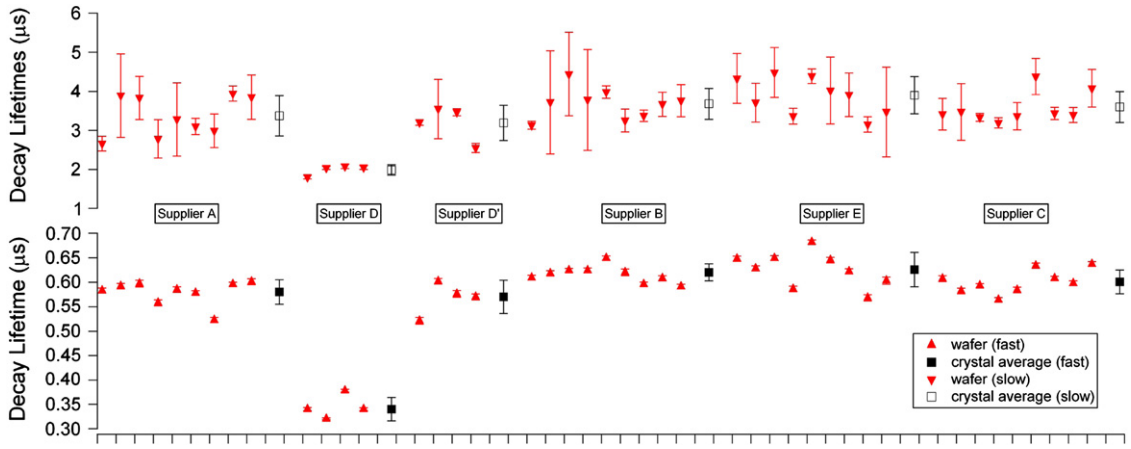

Fig. 4. Measured decay lifetimes of the fast (~0.6 μs; up triangles) and intermediate (~3.3 μs; down triangles) components for all 44 samples, with error bars reported from the fit procedure. The average decay lifetime of each crystal (squares) is also plotted along with the error bars representing the standard deviation. Evidence for a long-lived (~10 μs) component was primarily confined to the D wafers and was thus omitted from this plot.

Table 1
Impurities in ppm by sample from separate WD and EDXRF measurements. Though EDXRF measurements suggest the presence of Ag, Se and Au impurities, subsequent electron beam analyses of twelve wafers and WDXRF analyses of another six revealed no compelling evidence for the existence of these heavy impurities. Ultimately, their uniformity prevents correlations from being established. Likewise, the presence of S and Cl may be an artifact of sample preparation prior to the vacuum XRF analysis. Further, the S and Cl impurities definitively identified in the WDXRF measurements may have their ultimate origins in the optical coupling grease or solvents used to prepare the six samples for WDXRF measurements.

Supplier	WDXRF	WDXRF	WDXRF	WDXRF	EDXRF	EDXRF	EDXRF	EDXRF	EDXRF
	Na	S	Cl	Tl	A	Pt	Se	Au	Tl
A					70	< 11	22	50	159
A					62	< 11	21	65	173
A					57	< 11	33	72	141
A					76	< 11	26	88	147
A					75	< 11	21	43	177
A	< 50	403	233	452	58	< 11	19	126	154
A					84	< 11	52	98	143
A					80	< 11	55	74	127
A					83	< 11	29	92	130
AVE					72	NA	31	79	150
STDEV					10	NA	14	26	17
B					48	< 11	21	64	293
B					44	< 11	44	61	264
B					74	< 11	40	59	210
B	< 50	937	168	981	72	< 11	24	64	306
B					54	< 11	43	82	283
B					75	< 11	43	82	283
B					85	< 11	23	78	326
B					60	< 11	24	58	309
B					63	< 11	19	41	293
AVE					64	NA	29	69	289
STDEV					14	NA	10	21	35
C					76	< 11	22	67	231
C					96	< 11	27	73	238
C	< 50	803	< 20	989	86	< 11	34	96	290
C					49	< 11	29	102	258
C					102	< 11	40	133	286
C					60	< 11	22	39	239
C					86	< 11	30	88	259
C					60	< 11	21	51	257
C					94	< 11	34	56	257
AVE					79	NA	29	78	257
STDEV					19	NA	6	29	20
D	< 50	256	136	< 5	102	< 11	24	95	< 11
D					52	16	25	95	< 11
D					74	21	32	124	< 11
D					63	< 11	33	89	< 11
AVE					73	18	29	101	NA
STDEV					21	4	5	16	NA
D′					58	< 11	25	47	185
D′	< 50	647	102	893	53	< 11	25	62	395

Table 1 (*continued*)

Supplier	WDXRF	WDXRF	WDXRF	WDXRF	EDXRF	EDXRF	EDXRF	EDXRF	EDXRF
	Na	S	Cl	Tl	A	Pt	Se	Au	Tl
D′					80	< 11	23	58	426
D′					60	< 11	24	53	598
AVE					63	NA	24	55	401
STDEV					23	NA	1	6	169
E	< 50	546	140	1800	80	< 11	23	53	518
E					57	< 11	22	201	559
E					58	< 11	22	75	561
E					77	< 11	21	44	515
E					60	< 11	19	141	407
E					62	< 11	32	49	455
E					86	< 11	23	63	458
E					80	< 11	24	42	563
E					68	< 11	26	127	516
AVE					70	NA	24	88	506
STDEV					11	NA	4	56	55

the wafers using the same mechanical mounting rig shown in Fig. 2. Pixie-4 DSP code was modified to allow for high frequency sampling of short decay components and lower frequency sampling of longer decay components to accommodate (unknown) decay component waveforms as long in duration as ~100 us. The waveforms were fit with a triple exponential function to recover the fast, intermediate and slow decay components (0.6, 3.3 and 10 μs, respectively).

2.3. XRF

All 44 wafers were sent to Matrix Metrologies (El Granada, CA) for energy dispersive XRF measurements. Six of these wafers (one from each bulk crystal) were sent to Material Characterization Services (Austin, TX) for high precision wavelength dispersive XRF measurements.

3. Results

Results from the nonproportionality, energy resolution and decay lifetime measurements performed on the individual wafers are grouped by supplier in Figs. 3 and 4. Results from the XRF measurements are contained in Table 1. No statistically significant variation in nonproportionality, energy resolution or decay lifetimes is observed among wafers cut from the same bulk crystal. This uniformity prompted an alternative analysis wherein each wafer from the same bulk crystal is treated as an independent sample of bulk crystal properties. With this approach, individual nonproportionality, energy resolution and decay lifetime measurements are statistically combined to extract average properties for each bulk crystal. Fig. 4 also contains the results of this averaging procedure for the decay lifetimes, while Fig. 5 separately contains the combined nonproportionality and energy resolution results. When examined at the bulk crystal level it is manifestly evident that five of the six crystals are essentially indistinguishable from one another (within measurement error). In a similar vein, the crystal from supplier D is clearly an anomaly with the poorest energy resolution (~9.0%) and the shortest decay lifetimes of any of the other five crystals. Presumably, these differences are explained by the results of the EDXRF measurements (Table 1), which reveal no evidence of Tl (or Na) in this same crystal. (The non-detection of Tl (or Na) is somewhat surprising since the general shape of its nonproportionality curve is still reminiscent of CsI(Tl).) Presumably, the doping level in the crystal from supplier D is far from optimal for the wafer size (before cutting this crystal showed the best energy resolution of ~6.4%). The Tl doping level variations from ~150 to ~500 ppm (WDXRF results) exhibited by the other crystals do not seem to have an effect on nonproportionality or energy resolution.

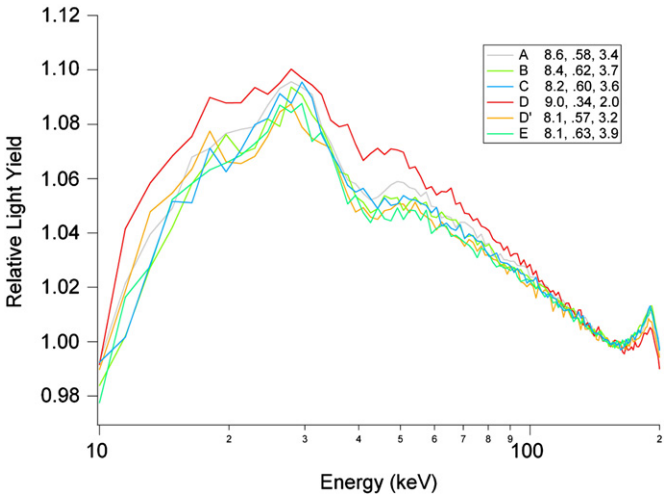

Fig. 5. Average nonproportionality curves derived from the individual curves for each crystal in Fig. 3. The very low Tl doping level is presumably responsible for the distinct correlations among nonproportionality, energy resolution and decay lifetimes in the D crystal.

4. Conclusions

Modern CsI(Tl) growth techniques are apparently capable of consistently producing very high purity crystal stock, with even the small (~10%) variation measured among NaI(Tl) crystals from different suppliers [3] apparently suppressed in CsI(Tl). There is little evidence in the work described herein to support the proposal that CsI(Tl) nonproportionality can be engineered via judicious control of impurities above the 50 ppm level (50 ppm for Na down to 1 ppm or less for Tl and heavy impurities) to improve its energy resolution. However, it is possible that impurities and/or the Tl dopant are controlled by supplier D at a very low level to achieve the excellent resolution measured in the bulk crystal. Resolution of this conundrum must await

analysis by more precise methods, including particle induced X-ray emission, neutron activation or mass spectrometry.

Acknowledgments

This work is based on the work sponsored by the US Department of Energy under Award no. DESC0001802.

References

[1] M. Moszyński, et al., IEEE Transactions on Nuclear Science NS-55 (2008) 1062.
[2] W. Hennig, et al., Journal of Radioanalytical and Nuclear Chemistry 282 (2009) 681.
[3] G. Hull, et al., IEEE Transactions on Nuclear Science, NS-26 (2006) 331 (200967 p31).